DALTON
FULL PAPER

Reactivity of the molybdenacarbaborane anion [2,2,2,2-$(CO)_4$-*closo*-2,1-$MoCB_{10}H_{11}$]$^-$: metal oxidation *versus* cage substitution †

Shaowu Du, Jason A. Kautz, Thomas D. McGrath and F. Gordon A. Stone *

Department of Chemistry and Biochemistry, Baylor University, Waco, TX 76798-7348, USA

Received 12th June 2001, Accepted 12th July 2001
First published as an Advance Article on the web 10th September 2001

In CH_2Cl_2 solutions, the Mo^{II} salt [$N(PPh_3)_2$][2,2,2,2-$(CO)_4$-*closo*-2,1-$MoCB_{10}H_{11}$] **1** is oxidized by iodine (1 equiv.) in the presence of $CNBu^t$ (4 equiv.) affording the Mo^{IV} complex [2,2,2,2-$(CNBu^t)_4$-2-I-*closo*-2,1-$MoCB_{10}H_{11}$], the structure of which was established by X-ray diffraction. In contrast, under similar conditions the corresponding tungsten salt yields a mixture of [2,2,2-$(CNBu^t)_3$-2-CO-2-I-*closo*-2,1-$WCB_{10}H_{11}$] and [2,2-$(CNBu^t)_2$-2,2-$(CO)_2$-2-I-*closo*-2,1-$WCB_{10}H_{11}$]. Treatment of **1** with iodine in tetrahydrofuran yields the Mo^{II} species [$N(PPh_3)_2$][2,2,2-$(CO)_3$-2-I-7-{$O(CH_2)_4$}-*closo*-2,1-$MoCB_{10}H_{10}$], the structure of which was also confirmed by X-ray diffraction. The latter with iodine and $S(CH_2)_4$ gives [2,2,2-$(CO)_3$-2-I-3-{$S(CH_2)_4$}-11-{$O(CH_2)_4$}-*closo*-2,1-$MoCB_{10}H_9$]. Using CH_2Cl_2 as solvent, **1** reacts with thioethers L [L = $S(CH_2)_4$, *cyclo*-1,4-$S_2(CH_2)_4$, *cyclo*-1,4,7-$S_3(CH_2)_6$, *cyclo*-1,4,7,10-$S_4(CH_2)_8$] and iodine to form [2,2,2-$(CO)_3$-2,3-μ-I-*n*-L-*closo*-2,1-$MoCB_{10}H_9$] (isomers, n = 7 and 11) and [2,2,2-$(CO)_3$-2-I-3,11-L_2-*closo*-2,1-$MoCB_{10}H_9$] [except L = *cyclo*-1,4,7,10-$S_4(CH_2)_8$]. The molecular structures of [2,2,2-$(CO)_3$-2,3-μ-I-7-{*cyclo*-1,4,7-$S_3(CH_2)_6$}-*closo*-2,1-$MoCB_{10}H_9$] and [2,2,2-$(CO)_3$-2-I-3,11-{*cyclo*-1,4-$S_2(CH_2)_4$}$_2$-*closo*-2,1-$MoCB_{10}H_9$] were determined by X-ray diffraction, confirming both to have doubly *B*-substituted cages and the former to contain a novel iodide bridge between molybdenum and a cage-boron atom.

The chemistry of transition metal complexes pentahapto coordinated by [*nido*-7-$CB_{10}H_{11}$]$^{3-}$ ligands has received very little attention since a few species of this class were first described several years ago.[1] The neglected study of monocarbollide metal complexes is surprising in view of the existence of numerous compounds having a metal atom similarly coordinated by the isolobally mapped dicarbollide ligand [*nido*-7,8-$C_2B_9H_{11}$]$^{2-}$ or its *C*-alkyl derivatives.[2] Moreover, monocarbollide metal complexes would be expected to display reactivity patterns distinct from those having dicarbollide groups on account of the different formal negative charges in the trianion [*nido*-7-$CB_{10}H_{11}$]$^{3-}$ and dianion [*nido*-7,8-$C_2B_9H_{11}$]$^{2-}$. We have thus begun to synthesize and develop the chemistry of several complexes with metal atoms bound on one side by a [*nido*-7-$CB_{10}H_{11}$]$^{3-}$ group and on the other by CO, phosphine or isocyanide ligands.[3]

The different reactivity patterns displayed by complexes having [*nido*-7-$CB_{10}H_{11}$]$^{3-}$ ligands from those with [*nido*-7,8-$C_2B_9H_{11}$]$^{2-}$ groups are illustrated by the nature of the products isolated upon treatment of salts of the anions [3,3,3-$(CO)_3$-*closo*-3,1,2-$ReC_2B_9H_{11}$]$^-$ and [2,2,2-$(CO)_3$-*closo*-2,1-$ReCB_{10}H_{11}$]$^{2-}$ with electrophilic transition metal fragments. Salts of the dianionic rhenium species afford heterodimetallic compounds with direct metal–metal bonds augmented by exopolyhedral B–H⟶M linkages, whereas salts of the monoanion yield zwitterionic molecules in which an electrophilic metal moiety is exopolyhedrally attached to the cage by one, two or three B–H⟶M bonds, and there is no direct bond between rhenium and the metal M.[3b,3c,4]

Salts of the monoanionic complexes [2,2,2,2-$(CO)_4$-*closo*-2,1-$MCB_{10}H_{11}$]$^-$ (**1**, M = Mo; **2**, M = W), or their derivatives in which a CO group is replaced by a PPh_3 molecule, also readily react with electrophilic reagents.[3d,e,h] Thus the molybdenum compound [$N(PPh_3)_2$][2,2,2-$(CO)_3$-2-PPh_3-*closo*-2,1-$MoCB_{10}H_{11}$] yields the zwitterionic *exo-closo* complexes [2,2,2-$(CO)_3$-2-PPh_3-7,8,12-$(\mu\text{-H})_3$-7,8,12-{$RuCl(PPh_3)_2$}-*closo*-2,1-$MoCB_{10}H_8$] and [2,2,2-$(CO)_3$-2-PPh_3-12-(μ-H)-12-{$Fe(CO)_2(\eta\text{-}C_5Me_5)$}-*closo*-2,1-$MoCB_{10}H_{10}$], respectively, in reactions with [$RuCl_2(PPh_3)_3$]/Tl[PF_6] and [$Fe(CO)_2(THF)(\eta\text{-}C_5Me_5)$][$BF_4$] (THF = tetrahydrofuran).[3e] In a further type of reaction involving BH vertices, treatment of salts of the anions [2,2,2-$(CO)_3$-2-PPh_3-*closo*-2,1-$MCB_{10}H_{11}$]$^-$ with $S(CH_2)_4$ and H_2SO_4 or CF_3SO_3Me affords the charge-compensated complexes [2,2,2-$(CO)_3$-2-PPh_3-7-{$S(CH_2)_4$}-*closo*-2,1-$MCB_{10}H_{10}$].[3h] Thus the anionic charge on the precursor is manifested by strong hydridic character of the B–H bonds. Electrophiles such as H^+ or Me^+ do not attach themselves to the metal centre but instead behave as hydride abstracting agents. If donor molecules are present neutral zwitterionic species result in which a boron-bound H^- is replaced by the donor molecule. In this manner ethers, dialkyl sulfides, nitriles, isocyanides and imines have been attached to the cage system.[3d,h] Moreover, elaboration of the *B*-functionality has been achieved by simple chemical transformation of the cage-bound groups, giving substituents such as amines and aldehydes bound to cluster boron vertices. These derivatization processes generally also incorporate at least one chiral centre into the molecule.

In seeking to extend further the chemistry of the monocarbollide complexes of molybdenum and tungsten, it was recognized that the high anionic charge of the ligand [*nido*-7-$CB_{10}H_{11}$]$^{3-}$ should stabilize these metals in oxidation states higher than the formal +II state of the compounds discussed above. We report herein the results of oxidizing **1** and **2** with iodine in the presence of donor ligand types. It was anticipated that the lesser back-bonding ability of the molybdenum and

† The compounds described herein have molybdenum (or tungsten) atoms incorporated into *closo*-1-carba-2-metalladodecaborane frameworks, and several have exopolyhedral substitutents. It should be noted that these substituted compounds, although containing chiral centres, here occur as racemates. For a 7-(ligand)-substituted species, an 11-(ligand) notation is equally valid; and for 3,7- and 3,11-disubstituted molecules, 6,11- and 6,7-descriptors, respectively, would also be correct. In each case the former is used in formulae, according to IUPAC convention.

Electronic supplementary information (ESI) available: crystal data for **15**. See http://www.rsc.org/suppdata/dt/b1/b105158j/

DOI: 10.1039/b105158j

This journal is © The Royal Society of Chemistry 2001

tungsten centres in oxidation states above +II would disfavour ligation of CO groups, and hence there was a perceived need for other donors to be present during oxidation. The choice of added donor ligand was limited by the necessity for compatibility with I_2: organophosphines, for example, could not be used, but isocyanides, ethers and thioethers all proved to be suitable substrates, and revealed some discrimination in behaviour according to the nature of the donor used.

Results and discussion

Reactions with CNBu^t and iodine: metal oxidation

When the Mo^{II} molybdenacarbaborane **1** was treated in CH_2Cl_2 with CNBu^t (4 molar equivalents) and I_2 (1 molar equivalent) at ambient temperatures the neutral Mo^{IV} species [2,2,2,2-(CNBu^t)$_4$-2-I-*closo*-2,1-$MoCB_{10}H_{11}$] **3** was obtained in excellent yield (Scheme 1). The analogous bromide complex **4** was formed similarly using Br_2 rather than I_2. Employing less than 4 equivalents of CNBu^t in the reaction of **1** with I_2 as expected resulted in incomplete substitution of all the metal-bound CO ligands. Interestingly, however, use of only 2 equivalents of the isocyanide yields the tris(isocyanide) species [2,2,2-(CNBu^t)$_3$-2-CO-2-I-*closo*-2,1-$MoCB_{10}H_{11}$] **5** as the only metallacarbaborane product. Moreover, using 3 equivalents of CNBu^t did not improve the yield of **5** but instead gave a mixture of **3** and **5**. In contrast with these results, similar treatment of the tungsten species **2** with 4 equivalents of CNBu^t and 1 equivalent of I_2 gave a mixture of [2,2,2-(CNBu^t)$_3$-2-CO-2-I-*closo*-2,1-$WCB_{10}H_{11}$] **6**, the analogue of **5**, and the bis(isocyanide) complex [2,2-(CNBu^t)$_2$-2,2-(CO)$_2$-2-I-*closo*-2,1-$WCB_{10}H_{11}$] **7**. Indeed, even with a large excess of the CNBu^t, only compounds **6** and **7** were observed and there was no evidence for formation of a fully isocyanide-substituted species analogous to **3**.

Data characterizing compounds **3**–**7** are given in Tables 1 and 2. Although spectroscopic analysis of **3** revealed that all molybdenum-bound carbonyl groups had been lost, and integrated ^{1}H NMR spectroscopy suggested the presence of four isocyanide ligands, the detailed constitution of **3** was not definitively established until an X-ray diffraction study was performed. A perspective view of the molecule is shown in Fig. 1. Full listings of bond distances and angles for this molecule, and for the others reported herein which were studied by X-ray diffraction, have been deposited as Electronic Supplementary Information. In **3** the metal is bonded on one side by the $\overline{CBBBB}$ open face of the *nido*-7-$CB_{10}H_{11}$ group and on the other by an iodide ion and by four CNBu^t ligands, the latter all in an essentially linear manner. If the open pentagonal face is regarded as a tridentate ligand, as is customary, the metal centre is 8-coordinated. The iodide ligand is sited *trans* to the centroid of the $\overline{CBBBB}$ face (I–Mo–CB_4 = 179.2°) with Mo–centroid = 1.877 Å and Mo–I = 2.9241(9) Å. The latter bond distance is perceptibly longer than that in the isolobal dication [MoI(CNBu^t)$_4$(η-C_5H_5)]$^{2+}$ [2.862(1) Å][5a] and Mo–I distances usually found (2.841 Å) in other 8-coordinate molybdenum compounds.[5b]

The NMR data for **3** (Table 2) are entirely consistent with the results of the structure determination, and hence the compositions and structures of molecules **4**–**7** could be inferred from that of **3** from comparison of their spectroscopic parameters. All five compounds display very similar ^{11}B{^{1}H} NMR spectra, showing six resonances in ratios of 1 : 2 : 1 : 2 : 2 : 2 (some peaks are coincident), respectively, reflecting their molecular mirror symmetry. There is also a general deshielding of the ^{11}B NMR signals compared with the corresponding data for **1**[3d] or **2**,[3h] consistent with the higher formal oxidation state of the metal centre. In the ^{1}H NMR spectrum of each of **3**–**7** there is a

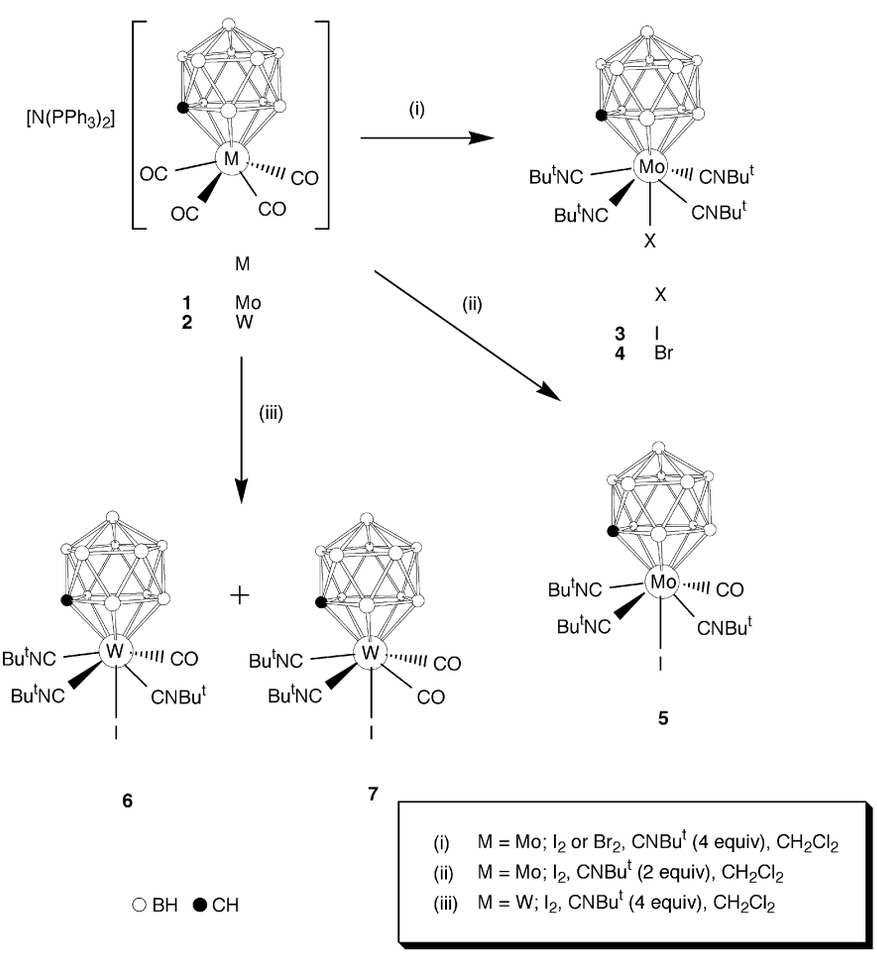

Scheme 1 Reactions of **1** and **2** in CH_2Cl_2 with I_2 and CNBu^t.

Table 1 Analytical and physical data

Compound	Yield (%)	ν_{max}(CO), ν_{max}(NC)* [a]/cm^{-1}	Analysis (%) [b,c] C	H
3 [2,2,2,2-(CNBu^t)$_4$-2-I-*closo*-2,1-MoCB$_{10}$H$_{11}$]	94	2198 w,* 2173 s*	37.4 (36.7)	7.0 (6.9)
4 [2,2,2,2-(CNBu^t)$_4$-2-Br-*closo*-2,1-MoCB$_{10}$H$_{11}$]	80	2206 w,* 2177 s*	39.4 (39.4)	7.1 (7.4)
5 [2,2,2-(CNBu^t)$_3$-2-CO-2-I-*closo*-2,1-MoCB$_{10}$H$_{11}$]	41	2207 w,* 2187 s,* 2037 s	28.9 (29.3) [d]	6.1 (5.4)
6 [2,2,2-(CNBu^t)$_3$-2-CO-2-I-*closo*-2,1-WCB$_{10}$H$_{11}$]	33	2211 w,* 2185 s,* 2027 s	28.5 (28.4)	5.3 (5.3)
7 [2,2-(CNBu^t)$_2$-2,2-(CO)$_2$-2-I-*closo*-2,1-WCB$_{10}$H$_{11}$]	18	2213 s,* 2205 s,* 2071 s, 2039 s	23.3 (23.5)	4.4 (4.4)
8 [N(PPh$_3$)$_2$][2,2,2-(CO)$_3$-2-I-7-{O(CH$_2$)$_4$}-*closo*-2,1-MoCB$_{10}$H$_{10}$]	37	2013 s, 1942 s, 1876 s	49.9 (50.4)	4.8 (4.6)
9 [2,2,2-(CO)$_3$-2,3-μ-I-*n*-{S(CH$_2$)$_4$}-*closo*-2,1-MoCB$_{10}$H$_9$] (n = 7, 11)	20	2033 s, 1975 w, 1927 m	19.2 (18.3)	3.4 (3.3)
10 [2,2,2-(CO)$_3$-2,3-μ-I-*n*-{*cyclo*-1,4-S$_2$(CH$_2$)$_4$}-*closo*-2,1-MoCB$_{10}$H$_9$] (n = 7, 11)	21	2034 s, 1976 w, 1926 m	19.4 (19.5) [e]	3.6 (3.4)
11 [2,2,2-(CO)$_3$-2,3-μ-I-*n*-{*cyclo*-1,4,7-S$_3$(CH$_2$)$_6$}-*closo*-2,1-MoCB$_{10}$H$_9$] (n = 7, 11)	35	2034 s, 1978 w, 1923 m	19.6 (19.5)	3.4 (3.4)
12 [2,2,2-(CO)$_3$-2,3-μ-I-*n*-{*cyclo*-1,4,7,10-S$_4$(CH$_2$)$_8$}-*closo*-2,1-MoCB$_{10}$H$_9$] (n = 7, 11)	48	2035 s, 1979 w, 1924 m	21.7 (21.3)	3.9 (3.7)
13 [2,2,2-(CO)$_3$-2-I-3,11-{S(CH$_2$)$_4$}$_2$-*closo*-2,1-MoCB$_{10}$H$_9$]	23	2020 s, 1950 s, 1932 s	23.0 (23.5)	4.3 (4.1)
14 [2,2,2-(CO)$_3$-2-I-3,11-{*cyclo*-1,4-S$_2$(CH$_2$)$_4$}$_2$-*closo*-2,1-MoCB$_{10}$H$_9$]	10	2020 s, 1950 s br	19.5 (19.9) [f]	3.5 (3.4)
15 [2,2,2-(CO)$_3$-2-I-3,11-{*cyclo*-1,4,7-S$_3$(CH$_2$)$_6$}$_2$-*closo*-2,1-MoCB$_{10}$H$_9$]	24	2020 s, 1949 s br	24.5 (24.1)	4.2 (4.2)
16 [2,2,2-(CO)$_3$-2-I-3-{S(CH$_2$)$_4$}-11-{O(CH$_2$)$_4$}-*closo*-2,1-MoCB$_{10}$H$_9$]	36	2021 s, 1952 s, 1934 m	21.3 (21.2)	4.1 (4.0)

[a] Measured in CH_2Cl_2; broad medium-intensity bands observed in the spectra of all compounds at *ca.* 2550 cm^{-1} are due to B–H absorptions. [b] Calculated values are given in parentheses. [c] Analyses for N: **3**, 8.1 (8.2%); **4**, 8.7 (8.8%); **5**, 6.2 (5.5%); **6**, 5.9 (5.8%); **7**, 4.2 (4.2%); **8**, 1.4 (1.3%). [d] Crystallizes with 1.5 mol equivalent of CH_2Cl_2. [e] Crystallizes with 0.5 mol equivalent of *cyclo*-1,4-S$_2$(CH$_2$)$_4$. [f] Crystallizes with 2.0 mol equivalent of CH_2Cl_2.

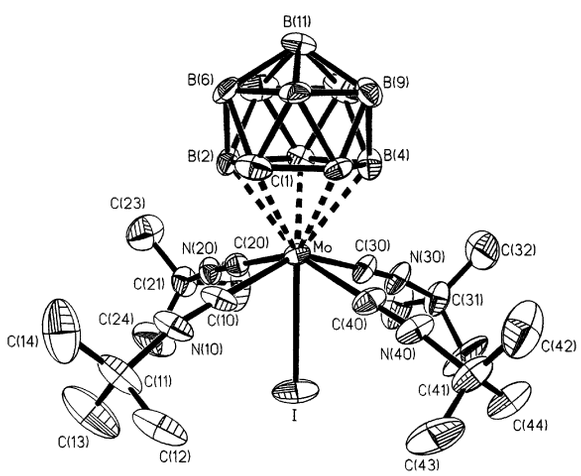

Fig. 1 Structure of **3** showing the crystallographic labeling scheme. In this and in Figs. 2–4 hydrogen atoms are omitted for clarity and thermal ellipsoids are drawn at the 40% probability level. Selected bond lengths (Å) and angles (°): Mo–B(3) 2.346(7), Mo–B(4) 2.380(8), Mo–B(2) 2.386(7), Mo–C(1) 2.437(6), Mo–B(5) 2.441(6), Mo–I 2.9241(9); C(30)–Mo–I 73.0(2), C(40)–Mo–I 73.5(2), C(10)–Mo–I 73.3(2), C(20)–Mo–I 73.7(2), B(3)–Mo–I 138.6(2), B(4)–Mo–I 140.2(2), B(2)–Mo–I 140.3(2), C(1)–Mo–I 144.2(2), B(5)–Mo–I 144.3(2).

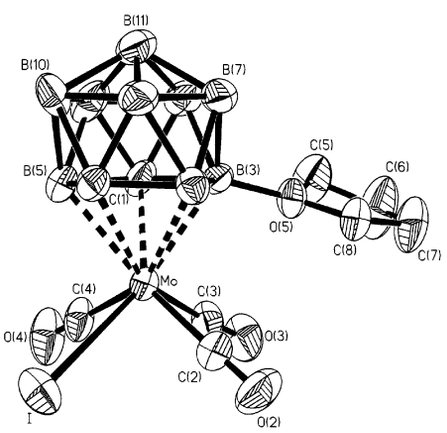

Fig. 2 Structure of **8** showing the crystallographic labeling scheme. Selected bond lengths (Å) and angles (°): Mo–B(4) 2.347(8), Mo–B(3) 2.349(8), Mo–B(5) 2.357(8), Mo–B(2) 2.390(7), Mo–C(1) 2.403(6), Mo–I 2.8839(8), B(3)–O(5) 1.558(8); C(3)–Mo–I 118.8(2), C(4)–Mo–I 75.5(2), C(2)–Mo–I 74.5(2), B(4)–Mo–I 140.3(2), B(3)–Mo–I 153.8(2), B(5)–Mo–I 96.7(2), B(2)–Mo–I 109.5(2), C(1)–Mo–I 85.9(2), O(5)–B(3)–Mo 112.5(4), O(2)–C(2)–Mo 178.0(7), O(3)–C(3)–Mo 176.1(7), O(4)–C(4)–Mo 176.2(7).

broad singlet resonance in the range δ 2.38 (**3**) to 2.77 (**7**), which is assigned to the cage CH unit. Correspondingly, in each of the $^{13}C\{^1H\}$ NMR spectra a broad resonance is seen for the cage C atom at δ 64.4 (**3**), 64.8 (**4**) and 66.2 (**5**) for the molybdenum species and slightly to higher field, at 57.2 (**6**) and 60.0 (**7**), for the tungsten compounds.

The Bu^t groups of the isocyanide ligands give rise to singlet resonances in the ^{1}H NMR spectra at around δ 1.5, with the number and intensity of the signals reflecting the molecular symmetry. Thus, in the spectra for **3** and **4**, only one peak of relative intensity 36 is seen, whereas two peaks with integrals 9 and 18 are found both for **5** and for **6**, and for **7** a single resonance of integral 18 is observed. Similar, symmetry-dictated patterns for the carbon atoms of the CNBu^t ligands of these complexes are also revealed in their $^{13}C\{^1H\}$ NMR spectra. The contact C atoms all appear as triplets [with J(NC) around 20 Hz], due to coupling with ^{14}N nuclei, and resonate around δ 140 when bound to molybdenum and at around δ 130 (with additional ^{183}W satellites) when coordinated to tungsten. Resonances assigned to the carbonyl groups in complexes **5**–**7** are observed at δ 209.7 (**5**), 199.1 (**6**) and 192.6 (**7**), these last two again showing additional structure due to coupling with the ^{183}W isotope. Evidently, the electron donating power of the isocyanide ligands is sufficient to enhance the electron density at the metal centre, thereby stabilizing the M^{IV}–CO linkage in **5**–**7**.

Molybdenum and tungsten carbaborane complexes closely related to compounds **3**–**7** have been reported.[6] Treatment of the anions [1,2-μ-NHBu^t-2,2,2-(CO)$_3$-*closo*-2,1-MCB$_{10}$H$_{10}$]$^-$ (M = Mo, W) with CNBu^t and I$_2$ gives [1,2-μ-NHBu^t-2,2,2-(CNBu^t)$_3$-2-I-*closo*-2,1-MCB$_{10}$H$_{10}$] species. These are similar to **3** save that the intramolecular μ-NHBu^t linkage of the parent compounds is retained in the products. In the tungsten system a second product was also formed, namely [1-NHBu^t-2,2-(CNBu^t)$_2$-2,2-(CO)$_2$-2-I-*closo*-2,1-WCB$_{10}$H$_{10}$], which is directly related to **7**, with the hydrogen bound to the cage-carbon atom

Table 2 ^{1}H, ^{13}C, and ^{11}B NMR data[a]

Compound	^{1}H δ[b]	^{13}C δ[c]	^{11}B δ[d]
3	2.38 (br s, 1 H, cage CH), 1.48 (s, 36 H, Bu^t)	150.2 [t, CN, *J*(NC) = 19], 64.4 (br, cage C), 58.1 (*C*Me_3), 29.7 (C*Me*$_3$)	11.4 (1 B), 5.0 (2 B), −6.1 (3 B), −6.9 (2 B), −15.3 (2 B)
4	2.43 (br s, 1 H, cage CH), 1.49 (s, 36 H, Bu^t)	153.2 [t, CN, *J*(NC) = 19], 64.8 (br, cage C), 58.0 (*C*Me_3), 29.9 (C*Me*$_3$)	11.4 (1 B), 5.3 (2 B), −6.2 (3 B), −7.0 (2 B), −15.3 (2 B)
5	2.53 (br s, 1 H, cage CH), 1.55 (s, 9 H, Bu^t), 1.48 (s, 18 H, Bu^t)	209.7 (CO), 143.5 [t, CN × 2, *J*(NC) = 19], 143.3 [t, CN, *J*(NC) = 18], 66.2 (br, cage C), 59.1 (*C*Me_3 × 2), 58.9 (*C*Me_3), 29.5 (C*Me*$_3$ × 2), 29.4 (C*Me*$_3$)	14.8 (1 B), 4.8 (2 B), −5.3 (5 B), −14.1 (2 B)
6	2.46 (br s, 1 H, cage CH), 1.56 (s, 9 H, Bu^t), 1.49 (s, 18 H, Bu^t)	199.1 [CO, *J*(WC) = 117], 134.9 [t, CN × 2, *J*(NC) = 21, *J*(WC) = 108], 134.2 [t, CN, *J*(NC) = 21, *J*(WC) = 100], 59.2 (*C*Me_3 × 2), 59.0 (*C*Me_3), 57.2 (br, cage C), 29.7 (C*Me*$_3$ × 2), 29.5 (C*Me*$_3$)	11.2 (1 B), −0.8 (2 B), −6.5 (1 B), −7.9 (2 B), −9.9 (2 B), −16.3 (2 B)
7	2.77 (br s, 1 H, cage CH), 1.56 (s, 18 H, Bu^t)	192.6 [CO, *J*(WC) = 117], 128.8 [t, CN, *J*(NC) = 20, *J*(WC) = 102], 60.4 (*C*Me_3), 60.0 (br, cage C), 29.5 (Me)	14.3 (1 B), −2.2 (2 B), −6.2 (3 B), −9.9 (2 B), −15.0 (2 B)
8	7.68–7.45 (m, 30 H, Ph), 4.05 (br m, 4 H, OCH_2), 2.15 (br s, 1 H, cage CH), 2.00 (br m, 4 H, CH_2)	250.2, 234.5, 231.3 (CO × 3), 134.1–126.8 (Ph), 78.5 (OCH_2), 55.8 (br, cage C), 25.0 (CH_2)	*22.6 (1B), −4.8 (2 B), −8.4 (1 B), −10.6 (2 B), −13.3 (1 B), −15.1 (1 B), −18.8 (1 B), −21.4 (1 B)
9[e]	3.64–3.06 (m, 8 H, SCH_2), 2.79, 2.58 (br s × 2, 1 H × 2, cage CH × 2), 2.28–1.99 (m, 8 H, CH_2)	229.8, 228.4, 228.2, 224.4, 223.5, 221.3 (CO × 6), 52.9, 50.0 (br, cage C × 2), 45.3, 44.4, 44.1, 43.0 (SCH_2 × 4), 31.4, 31.1, 30.2, 30.0 (CH_2 × 4)	*10.3 (1 B), *8.8 (1 B), 3.9 (2 B), 3.4 (2 B), −2.9 (3 B), −7.6 (1 B), −9.2 (1 B), −13.3 (3 B), −14.6 (1 B), −15.9 (1 B), −17.4 (2 B), −18.0 (2 B)
10[e]	3.35–2.84 (m, 16 H, SCH_2), 2.78, 2.61 (br s × 2, 1 H × 2, cage CH × 2)	229.5, 228.8, 228.7, 224.2, 223.0, 221.0 (CO × 6), 52.7, 49.9 (br, cage C × 2), 40.7, 39.7, 39.3, 39.2 (B–SCH_2), 27.5, 27.2, 26.8, 26.6 (SCH_2)	*10.1 (1 B), *7.6 (1 B), 3.4 (1 B), 2.9 (1 B + *1 B), *1.8 (1 B), −2.7 (1 B), −3.4 (3 B), −7.6 (1 B), −10.0 (1 B), −12.8 (2 B), −13.4 (1 B), −14.0 (1 B), −16.8 (1 B), −17.9 (3 B)
11[f]	3.78–2.62 (m, 13 H, CH_2 and cage CH)	†229.7, †228.7, 228.5, 224.3, †222.9, 221.1 (CO × 6), 52.9, †50.2 (br, cage C × 2), 44.1 (B–SCH_2), 37.5, 36.0, 32.6, 32.1 (CH_2)	†,*10.3, *8.4 (1 B), 3.7 (1 B), *3.6 (1 B), −2.7 (2 B), −7.7 (1 B), †−9.2, −12.8 (2 B), †−14.1, †−16.5, −17.9 (2 B)
12[f]	3.44–2.74 (m, 16 H, CH_2), 2.60 (br s, 1H, cage CH)	†229.9, †228.4, 228.3, 224.2, †223.1, 221.1 (CO × 6), 53.2, †50.1 (br, cage C × 2), 41.8, 41.4 (B–SCH_2), 32.4, 32.3, 32.0, 31.9, 31.5, 28.9, 28.3 (CH_2)	†,*10.2, *7.9 (1 B), 3.6 (1 B + *1 B), †3.1, †,*2.6, †−2.3, −3.0 (2 B), −7.8 (1 B), †−9.7, −12.7 (2 B), †−13.9, †−16.5, −17.7 (2 B)
13	3.65–3.03 (m, 9 H, SCH_2 and cage CH), 2.36–1.92 (m, 8 H, CH_2)	241.9, 226.7, 223.9 (CO × 3), 60.1 (br, cage C), 46.3, 45.1, 43.6, 43.2 (SCH_2 × 4), 31.0, 29.9, 29.9, 29.5 (CH_2 × 4)	*5.4 (1 B), −2.0 (1 B), −3.6 (1 B + *1 B), −8.1 (1 B), −10.8 (2 B), −12.2 (1 B), −16.9 (1 B), −17.9 (1 B)
14	3.66–2.87 (m, 17 H, SCH_2 and cage CH)	242.0, 226.6, 224.1 (CO × 3), 57.8 (br, cage C), 41.3, 40.5, 39.3, 39.1 (B–SCH_2 × 4), 27.3, 27.2, 26.9, 26.9 (SCH_2 × 4)	*3.8 (1 B), −3.0 (1 B), −5.2 (1 B), *−5.5 (1 B), −8.4 (1 B), −11.0 (2 B), −13.3 (1 B), −16.1 (1 B), −18.2 (1 B)
15	3.88–2.79 (m, 25 H, SCH_2 and cage CH)	242.2, 226.5, 224.8 (CO × 3), 57.8 (br, cage C), 46.3, 44.9, 44.5, 44.4 (B–SCH_2 × 4), 37.1, 37.0, 36.3, 35.9, 32.6, 32.2, 32.1, 31.7 (SCH_2 × 8)	*5.5 (1 B), −2.7 (1 B), −4.2 (1 B + *1 B), −8.4 (1 B), −10.9 (2 B), −13.5 (1 B), −15.9 (1 B), −17.7 (1 B)
16	3.64–3.04 (m, 8 H, OCH_2 and SCH_2), 2.99 (br s, 1 H, cage CH), 2.47–1.43 (m, 8 H, CH_2)	241.5, 227.9, 224.4 (CO × 3), 68.7 (OCH_2), 56.0 (br, cage C), 46.8, 43.5, 42.1 (OCH_2 and SCH_2 × 2), 31.1, 30.8, 30.1, 29.6 (CH_2 × 4)	*23.2 (1 B), *3.1 (1 B), −6.7 (1 B), −7.6 (1 B), −9.3 (1 B), −10.1 (1 B), −11.1 (1 B), −15.6 (1 B), −18.1 (1 B), −23.6 (1 B)

[a] Chemical shifts (δ) in ppm, coupling constants (*J*) in Hz, measurements at ambient temperatures in CD_2Cl_2. [b] Resonances for terminal BH protons occur as broad unresolved signals in the range δ *ca.* −1 to 3. [c] $^{13}C\{^{1}H\}$ decoupled chemical shifts (δ) are positive to high frequency of $SiMe_4$. [d] $^{11}B\{^{1}H\}$ decoupled chemical shifts (δ) are positive to high frequency of $BF_3{\cdot}Et_2O$ (external). Signals ascribed to more than one boron nucleus may result from overlapping peaks and do not necessarily indicate symmetry equivalence. Peaks marked with an asterisk are assigned to cage-boron nuclei carrying non-H substituents (see text) since they occur as singlets in fully coupled ^{11}B spectra. In some cases peak overlap in ^{11}B spectra obscures the resonance for a substituted boron and hence these cannot always unambiguously be assigned. [e] Occurs as a mixture of isomers (see text) in approximate ratio 1 : 1 (by integrated ^{11}B NMR spectroscopy); resonances for both isomers are discernible. [f] Occurs as a mixture of isomers (see text) in approximate ratio 7 : 1 (**11a** : **11b**) or 3 : 1 (**12a** : **12b**) (by integrated ^{11}B NMR spectroscopy); many minor isomer resonances are obscured: those which may be ascribed thereto are marked by †.

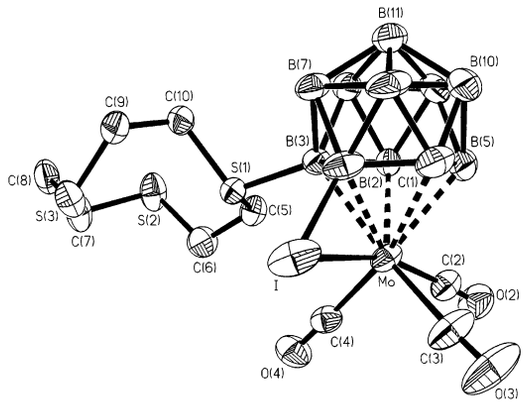

Fig. 3 Structure of **11a** showing the crystallographic labeling scheme. Selected bond lengths (Å) and angles (°): Mo–B(2) 2.262(7), Mo–C(1) 2.354(7), Mo–B(5) 2.377(10), Mo–B(3) 2.407(7), Mo–B(4) 2.433(8), Mo–I 2.8375(9), B(2)–I 2.193(9), B(3)–S(1) 1.905(7); C(4)–Mo–I 91.8(2), C(2)–Mo–I 163.4(2), C(3)–Mo–I 86.2(2), B(2)–Mo–I 49.4(2), C(1)–Mo–I 77.4(2), B(5)–Mo–I 117.6(2), B(3)–Mo–I 79.7(2), B(4)–Mo–I 119.8(2), I–B(2)–Mo 79.1(3), S(1)–B(3)–Mo 110.3(3), B(2)–I–Mo 51.5(2).

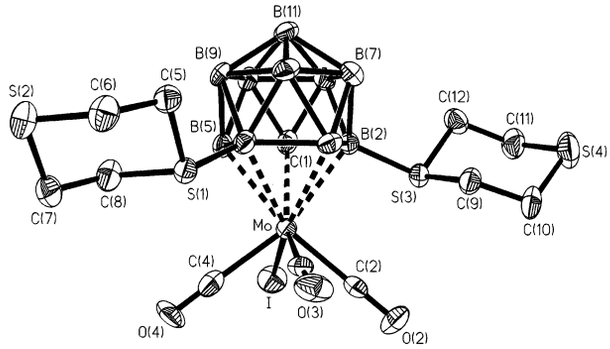

Fig. 4 Structure of **14** showing the crystallographic labeling scheme. Selected bond lengths (Å) and angles (°): Mo–B(4) 2.363(7), Mo–B(3) 2.370(8), Mo–B(5) 2.384(8), Mo–B(2) 2.396(8), Mo–C(1) 2.421(6), Mo–I 2.8693(8), B(2)–S(3) 1.917(8), B(4)–S(1) 1.936(8); C(3)–Mo–I 132.5(2), C(2)–Mo–I 75.0(2), C(4)–Mo–I 73.8(2), B(4)–Mo–I 137.2(2), B(3)–Mo–I 146.4(2), B(5)–Mo–I 93.7(2), B(2)–Mo–I 103.2(2), C(1)–Mo–I 79.5(2), S(3)–B(2)–Mo 106.5(3), S(1)–B(4)–Mo 109.2(4).

replaced by an NHBu^t group. It is notable that in **7** there is no evidence of isomerism in the metal-bound ligands, whereas the corresponding *C*-NHBu^t species exists as a mixture of two isomers with the carbonyl ligands believed to be mutually arranged either *cisoid* or *transoid* about the metal centre.[6]

Reactions with tetrahydrofuran or thioethers and iodine: cage substitution

Compound **1** displays an altogether different reactivity pattern upon treatment with iodine and ether or thioether ligands than that observed when the added ligand was *tert*-butyl isocyanide. Thus, the sole product isolated following treatment of a THF solution of **1** with one equivalent of I_2 was [N(PPh$_3$)$_2$][2,2,2-(CO)$_3$-2-I-7-{O(CH$_2$)$_4$}-*closo*-2,1-MoCB$_{10}$H$_{10}$] **8**, in which the carbaborane cage has undergone substitution at a boron vertex (Scheme 2). Data characterizing **8** are presented in Tables 1 and 2. The presence of a boron-bound THF moiety was immediately apparent following NMR spectroscopic analysis. In the ^{11}B{^{1}H} NMR spectrum, the presence of ten different resonances (with two pairs of coincidences) indicated a lowering of the symmetry of the carbaborane, and substitution was confirmed by the observation of a strongly deshielded resonance that remains a singlet upon retention of proton coupling. Its chemical shift, δ 22.6, is typical for ether-substituted boron vertices in such systems.[3d,h] Characteristic resonances for the THF moiety are also seen in the ^{1}H and ^{13}C{^{1}H} NMR spectra (^{1}H: δ 2.00, 4.05; ^{13}C: δ 25.0, 78.5), confirming the identity of the boron-bound substituent.

The site of attachment of the THF group, however, could not be determined solely by NMR spectroscopy and accordingly an X-ray diffraction structural study was performed, revealing the anion of **8** to have the geometry shown in Fig. 2. Substitution has taken place at a β boron atom in the C*B*B*B*B face which ligates the molybdenum atom in a normal pentahapto fashion. In **8**, as in the related species [2,2,2-(CO)$_3$-2-PPh$_3$-7-{O(CH$_2$)$_4$}-*closo*-2,1-MoCB$_{10}$H$_{10}$],[3d] the metal fragment is orientated such that the non-carbonyl ligand (I or PPh$_3$) on molybdenum is *transoid* to the substituted boron atom. The B–O distance [B(3)–O(5) 1.558(8) Å] is slightly longer than that [1.532(2) Å] in the aforementioned PPh$_3$-substituted species, perhaps simply as a consequence of the ionic nature of **8** and the differing substituents at the metal centre.

With thioether ligands and iodine compound **1** again reacts to form cage-substituted species but here the situation is rather more complicated than with THF. In CH_2Cl_2 solution, when **1** is treated with equimolar amounts of I_2 and thioethers L [L = S(CH$_2$)$_4$, *cyclo*-1,4-S$_2$(CH$_2$)$_4$, *cyclo*-1,4,7-S$_3$(CH$_2$)$_6$, *cyclo*-1,4,7,10-S$_4$(CH$_2$)$_8$], two distinct product types are formed (Scheme 2). The members of the first series are all of the general formulation [2,2,2-(CO)$_3$-2,3-μ-I-*n*-L-*closo*-2,1-MoCB$_{10}$H$_9$] and for each L are isolated as a mixture of two isomers [L = S(CH$_2$)$_4$, *n* = 7 (**9a**) or 11 (**9b**); L = *cyclo*-1,4-S$_2$(CH$_2$)$_4$, *n* = 7 (**10a**) or 11 (**10b**); L = *cyclo*-1,4,7-S$_3$(CH$_2$)$_6$, *n* = 7 (**11a**) or 11 (**11b**); L = *cyclo*-1,4,7,10-S$_4$(CH$_2$)$_8$, *n* = 7 (**12a**) or 11 (**12b**)], with the isomers differing in the boron atom to which the sulfur ligand is bound.

Data characterizing compounds **9**–**12** are given in Tables 1 and 2. Initial examination of the ^{11}B{^{1}H} NMR spectra obtained from these chromatographic fractions immediately showed each to be a mixture of two species. For both **9** and **10**, two isomers are formed in approximately equal amounts, but for compound **11** the ratio is approximately 7 : 1 and for **12** it is approximately 3 : 1. Comparison of their ^{11}B{^{1}H} NMR data also indicated that the same isomer is formed in the majority for both **11** and **12**. However, all attempts to further separate the two isomeric components of each mixture were unsuccessful, with the exception of compounds **11** for which one isomer is formed in much greater proportion than the other. Repeated fractional crystallization of this mixture ultimately afforded single crystals of exclusively the major isomer. An X-ray structure determination upon one of these crystals revealed the molecular structure shown in Fig. 3, in which an iodide ligand bound to the molybdenum centre is seen also to form an intramolecular bridge to one of the boron atoms of the carbaborane cage. To our knowledge, this feature is unprecedented in halo-metallacarbaborane chemistry.

The bridging iodide moiety links the metal vertex to an α boron atom in the coordinating C*B*BB*B* face of the carbaborane. Several of the associated geometric parameters are noteworthy: the Mo–I distance [2.8375(9) Å] is significantly shorter than that in **8**, and the angle Mo–I–B(2) is rather acute, at 51.5(2)°. Moreover, there is clearly some slippage of the Mo atom towards B(2) to accommodate the bridging interaction, with Mo–B(2) 2.262(7) Å. In this respect the system merits comparison with the structure determined for the anion [1,2-μ-NHBu^t-2,2,2-(CO)$_3$-*closo*-2,1-WCB$_{10}$H$_{10}$]$^-$,[6] in which an NHBu^t unit bridges between the cage-carbon atom and the tungsten with W–N–C 67.1(2)°, and again shows evidence of the metal vertex being somewhat slipped in order to satisfy the geometric constraints of the bridge.

A trithiane ligand is bonded to a cage boron atom in a site that is β with respect to the cage-carbon atom in the open CB*B*B face of the carbaborane ligand, with B(3)–S(1) 1.905(7) Å.

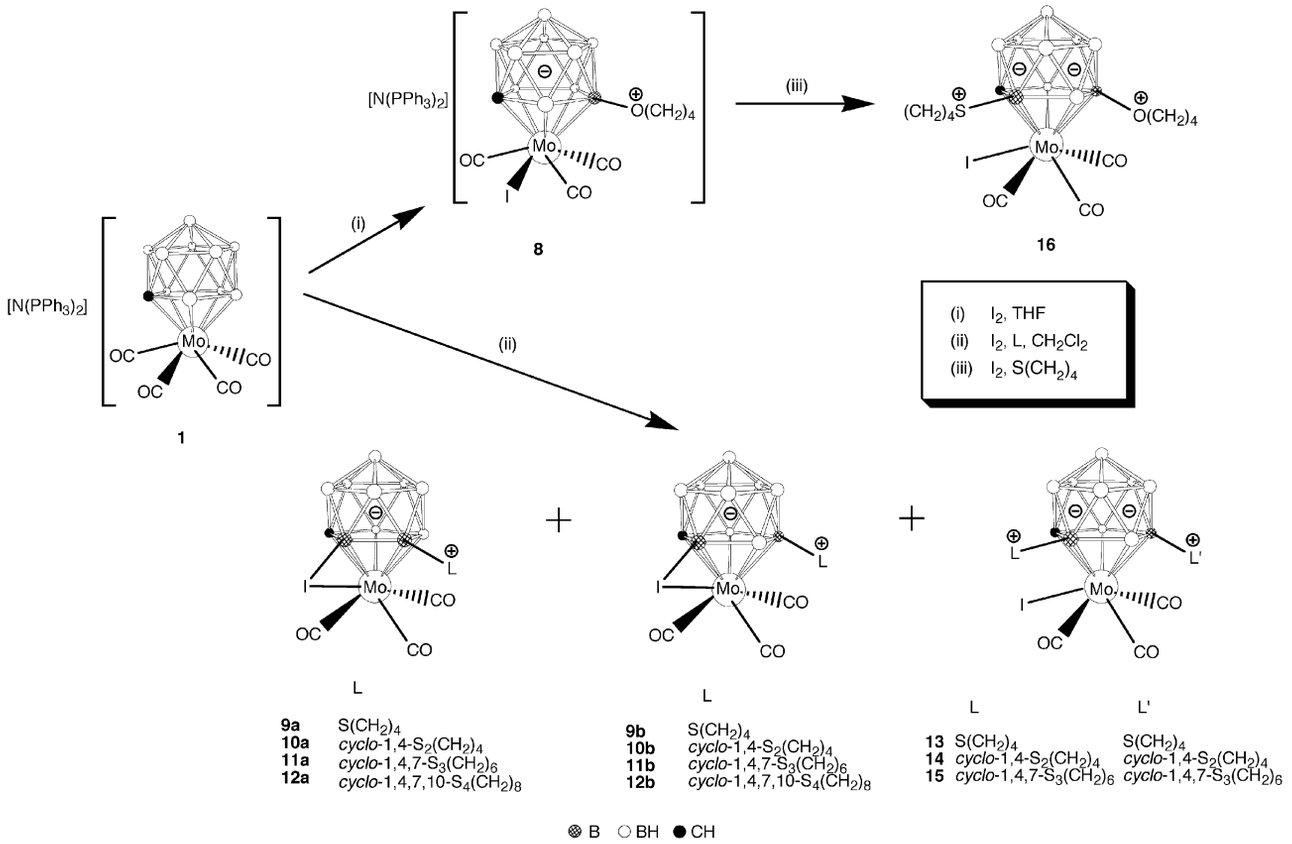

Scheme 2 Reactions of **1** with I_2 and ethers or thioethers.

This structural study establishes that this major isomer of compounds **11** is the 7-L-substituted compound **11a**. In **11a**, and likewise it may be assumed in the analogous compounds **9a**, **10a** and **12a**, the iodine and sulfur substituents are attached at adjacent sites, α and β respectively, of the carbaborane C*BB*BB face; whereas in the isomeric species **9b**–**12b** the substituents are located at the non-adjacent α and β′ boron atoms of the C*B*B*B*B belt. This formulation for **9b**–**12b** is reasonably inferred from the structure determined for **11a** and from consideration of the likely pathway by which **9**–**12** are formed, discussed below.

The $^{11}B\{^1H\}$ NMR spectra of the isomeric mixtures **9**–**12** are necessarily complicated by the isomerism and the absence of cluster symmetry. However, it did prove possible in some cases tentatively to locate the resonances due to the sulfur-substituted boron atom, in the range around δ 1–4. Signals due to the iodine-substituted boron vertices appear slightly to lower field, and are well separated from the remaining resonances, at δ *ca.* 10 (**9b**–**12b**) and δ *ca.* 8 (**9a**–**12a**). The ^1H and $^{13}C\{^1H\}$ NMR spectra of **9**–**12** are dominated by peaks due to the methylene units of the thioether ligands with, in addition, signals attributable to the cage CH units at around $\delta(^1H)$ 2.6 (**9a**–**12a**) and 2.8 (**9b**–**12b**) and $\delta(^{13}C)$ 50 (**9b**–**12b**) and 53 (**9a**–**12a**). Six resonances between δ 221 and 230 are also seen in the $^{13}C\{^1H\}$ NMR spectra, corresponding to the two sets of 3 CO ligands for each isomer. Interestingly, the one CO that is *transoid* to iodide at each molybdenum centre is not significantly deshielded relative to the other two, in contrast with the situation in compound **8** and also in **13**–**16** below.

It is noteworthy that the purple colour of compounds **9**–**12** is very similar to that of the anions [1,2-μ-NHBu^t-2,2,2-$(CO)_3$-*closo*-2,1-$MCB_{10}H_{10}]^-$ (M = Cr, Mo, W)[6] and is rather different from that of Mo^{II} compounds typified by **1**, which have conventional 'piano stool' configurations and which are generally red to yellow. Indeed, purple may be characteristic of the presence of the intramolecular bridge and perhaps arises from a necessary alteration in metal hybridization to accommodate the geometric demands of this feature.

The second series of products formed in the reaction of **1** with $\mathbf{I_2}$ and thioethers has the formulation [2,2,2-$(CO)_3$-2-I-3,11-L_2-*closo*-2,1-$MoCB_{10}H_9$] [L = $S(CH_2)_4$ **13**, *cyclo*-1,4-$S_2(CH_2)_4$ **14**, *cyclo*-1,4,7-$S_3(CH_2)_6$ **15**]. No product of this type was observed for L = *cyclo*-1,4,7,10-$S_4(CH_2)_8$ and the species **13**–**15** were obtained as single isomers. Although the composition of these compounds and the presence of two cage-bound sulfur ligands were readily deduced from their NMR data, an X-ray diffraction study was again necessary to establish their detailed configuration. Suitable crystals of compounds **14** and **15** were analysed; the resulting molecular structure of **14** is shown in Fig. 4. Compound **15** was found to be very similar to **14**, and the results of that study are included in the ESI only.

Compound **14** consists of a molybdenum centre which is bonded on one side by 3 CO ligands and an iodide and on the other by an 8,10-{*cyclo*-1,4-$S_2(CH_2)_4$}$_2$-*nido*-7-$CB_{10}H_9$ carbaborane moiety. The metal-to-carbaborane coordination is of conventional pentahapto type and the cage itself has undergone double substitution by the two sulfur ligands, at the α and β′ sites of the open C*BB*BB face. Significantly, these boron sites are the same positions that bear substituents in compounds **9b**–**12b** but no isomers of **13**–**15** were observed having a substitution pattern which mirrored that in **9a**–**12a**.

Data characterizing the molecules **13**–**15** are listed in Tables 1 and 2. The ^1H and $^{13}C\{^1H\}$ NMR spectra are again dominated by peaks due to the methylene groups of the sulfur ligands but are otherwise very similar. Resonances for the cage CH protons are obscured, but in the $^{13}C\{^1H\}$ NMR spectra the cage-carbon atom gives rise to a broad peak at δ 60.1 (**13**) and 57.8 (**14**, **15**). For each compound, three resonances for the CO ligands are seen, with one somewhat to higher field (δ *ca.* 242) than the other two (δ *ca.* 227, 224). In the $^{11}B\{^1H\}$ NMR spectra, ten resonances are seen (some are coincident), consistent with the

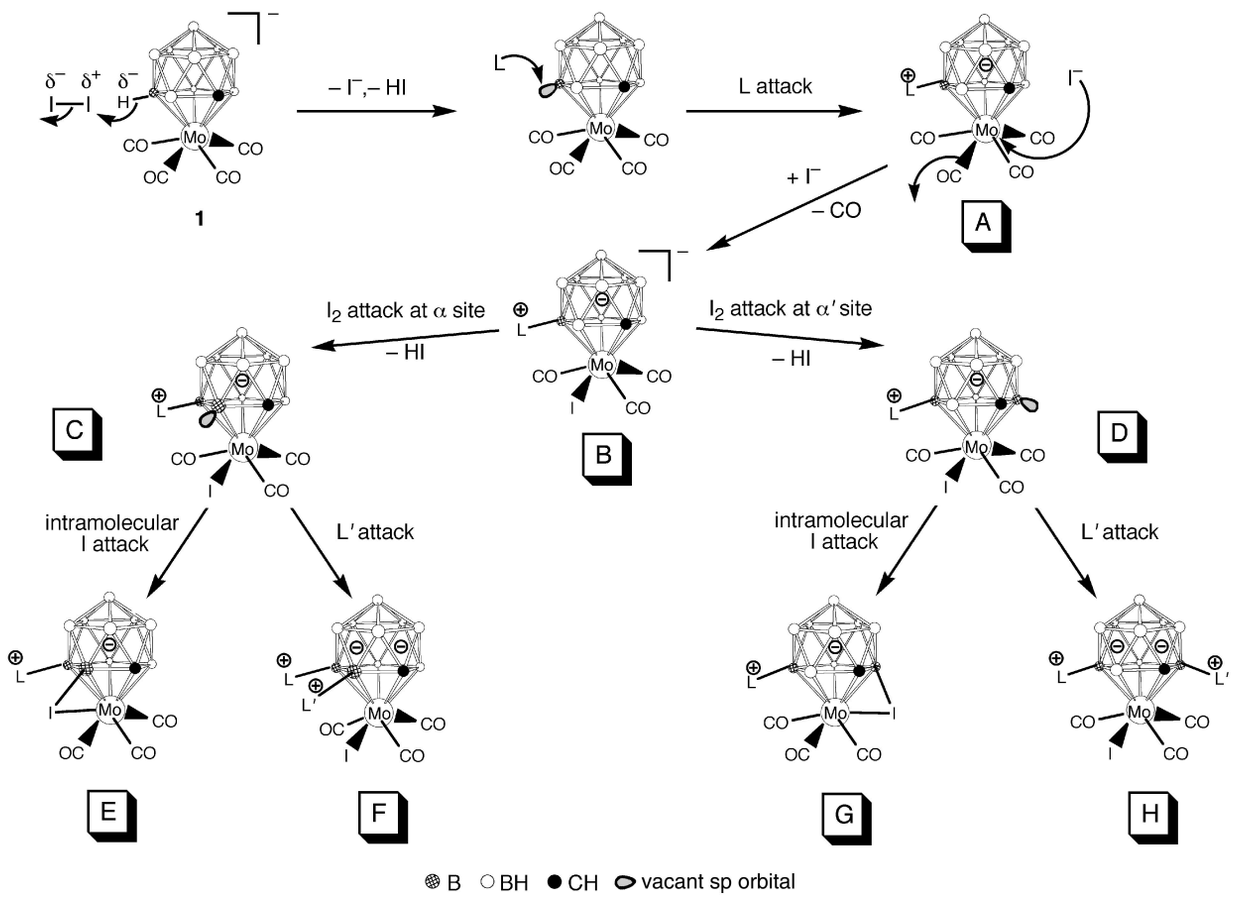

Scheme 3 Proposed pathway for the iodine-promoted formation of cage-substituted compounds **8**–**16**.

absence of molecular mirror symmetry arising from the αβ′ pattern of substitution: αα′ or ββ′ disubstitution of the cage would retain this symmetry. Those boron atoms which bear the thioether substitutents appear as singlets in fully-coupled ^{11}B NMR spectra, at around δ 5 and −4. However, it is not possible definitively to identify which resonance corresponds to which of the α or β′ boron atoms. Although the β-substituted boron atoms in compounds **9**–**12** resonate at around δ 3, the chemical shifts of such β-thioether-substituted boron vertices in {*closo*-2,1-MCB_{10}} systems have been observed[3d,g,h] between δ 3 and −3 and hence any such assignment here may be unreliable.

Mechanism of iodine-promoted boron vertex substitutions

The iodine-promoted replacement of boron-bound hydrides by two-electron donor molecules [eqn. (1)] may formally be regarded as an oxidative-substitution reaction.

$$B\text{–}H^- + I_2 + :L \longrightarrow B^{\delta-}\text{–}L^{\delta+} + H^+I^- + I^- \qquad (1)$$

Such processes have been observed previously: in thiadecaborane chemistry, the oxidative cluster closure of [*arachno*-$SB_9H_{12}]^-$ to *nido*-SB_9H_{11} by iodine was observed in the presence of donor solvents L instead to yield *arachno*-$SB_9H_{11}L$.[7] Eqn. (1) may also be compared with the reactions of carbaboranes[8] or carbametallaboranes[3d,3g,3h,9] whereby, for example, an added proton combines with a boron-bound hydride in the presence of donors to eliminate H_2 and boron substitution again takes place. The term 'oxidative-substitution' has earlier been coined by Hawthorne and co-workers with reference to closely-related reactions in which anionic carbaboranes are oxidized by $FeCl_3$ in the presence of donor ligands to afford the corresponding neutral, charge-compensated species with a B–H unit replaced by B–(ligand).[10]

In the present systems, the proposed pathway for formation of the compounds **8**–**15** is shown in Scheme 3. The anion of compound **1** is thought to undergo initially an oxidative-substitution process to give the charge-compensated intermediate **A**, substitution by the ligand L occurring at a β boron atom in the carbaborane C*B*B*B*B face, as is usual.[3d,g,h] For **A** the reduction in overall charge compared to **1** renders the Mo-bound CO ligands open to displacement by iodide giving **B** (*cf.* compound **8**). Anion **B** is susceptible to further attack by iodine (or, indeed, by protons from liberated HI), now at an α boron atom in the carbaborane C*B*BB*B* belt, removing a hydride to temporarily produce a 'naked' boron vertex. Because there are two possible, non-equivalent α sites for such an attack, two intermediates **C** and **D** can result. Two pathways are available to each of these intermediates to stabilize the naked boron vertex. From **C**, intramolecular lone-pair donation from the molybdenum-bound iodide into the vacant orbital on boron forms the iodine-bridged species **E** (*cf.* compounds **9a**–**12a**), whilst lone-pair donation from a further molecule of the donor L′ into this vacant orbital produces the doubly-zwitterionic molecule **F** (not observed experimentally). Similarly, the same two processes from intermediate **D** afford products **G** (*cf.* compounds **9b**–**12b**) and **H** (*cf.* compounds **13**–**15**), respectively.

In terms of this mechanism, it seems likely that compounds of type **F** are not formed simply on steric grounds or that they are formed but readily decompose to relieve intramolecular congestion, especially in the case of the more bulky polysulfur ligands. Moreover, other more subtle factors may be involved. In particular, the detailed electronic structure of the intermediate **B** may direct the site of electrophilic attack. For **C** and **D** the non-coordinated sulfur atoms of the polysulfur macrocycles may play a role in the delivery of iodine to the cluster, as thioethers are known to form charge-transfer complexes with halogens.[11] Indeed, such complex formation may play a role in initial activation (polarization) of the halogen. It is of interest

to note that when the salt **1** is treated with iodine in $S(CH_2)_4$ solution, compound **13** is the only observed product, formed in yields similar to the reaction described above. This might suggest that formation of the intermediate **D** proceeds more rapidly than production of **C**. Competitive reaction of **D** to give **G** or **H** could then progress exclusively along the latter pathway in the presence of vast excess of $S(CH_2)_4$. Indeed, an iodine–$S(CH_2)_4$ complex would be sterically hindered and this should significantly disfavour formation of an intermediate **C** in this case.

It is not clear why compound **8** does not react further with THF to afford a doubly-THF substituted species. One possible explanation may be the differing iodine complexation strength of oxygen *versus* sulfur donors, and an apparent consequent reduction in iodine reactivity in THF. When **8** is treated with further iodine in THF, no reaction is detected. However, treatment of **8** with iodine using $S(CH_2)_4$ as solvent results in a second cage substitution, suggesting that the iodine is more reactive in this medium. The product of this reaction is [2,2,2-$(CO)_3$-2-I-3-{$S(CH_2)_4$}-11-{$O(CH_2)_4$}-*closo*-2,1-$MoCB_{10}H_9$] **16**. It appears likely that the electron-withdrawing power of the boron-bound THF ligand and the molybdenum-bound iodide deactivates compound **8** relative to the parent **1**, but clearly **8** *is* susceptible to further substitution under suitable conditions.

Data characterizing compound **16** are given in Tables 1 and 2. Multiplet resonances due to the CH_2 units of the cage-bonded ligands are seen in typical positions in the ^{1}H and $^{13}C\{^1H\}$ NMR spectra, with the cage CH proton giving rise to a broad singlet at δ 2.99 and the cage-carbon atom resonating at δ 56.0. Peaks for the three CO ligands are seen in the $^{13}C\{^1H\}$ NMR spectrum at δ 241.5, 227.9 and 224.4, similar to those in **13**–**15**. In the $^{11}B\{^1H\}$ spectrum ten separate signals are seen, of which two remain singlets upon retention of proton coupling. These two peaks' positions are δ 23.2 and 3.1 and may be assigned as the B–$O(CH_2)_4$ and B–$S(CH_2)_4$ nuclei, respectively.

Conclusion

Several interesting results stem from the studies described herein. Whereas **1** does not by itself react directly with $CNBu^t$, ethers or thioethers at ambient temperatures,[3d,h] it does readily react with these donors in the presence of iodine. The nature of the products isolated thereafter depends greatly on whether the donor molecules present are those of $CNBu^t$ or those of a dialkyl sulfide or THF. With the isocyanide present, the metal is oxidized and the cage adopts its classical spectator role in the products. If sulfides or THF are present, however, the metal retains its formal M^{II} oxidation state but the carbaborane cage becomes mono- or di-substituted. The existence of the charge-compensated complex [2,2,2-$(CO)_3$-2-PPh_3-7-$CNBu^t$-*closo*-2,1-$MoCB_{10}H_{10}$][3h] derived from [2,2,2-$(CO)_3$-2-PPh_3-*closo*-2,1-$MoCB_{10}H_{11}$]$^-$ might suggest that the isocyanide can form species structurally akin to **A** of Scheme 3. Hence it seems in principle that if iodine and thioethers react with **1** according to Scheme 3 then $CNBu^t$ could do so also. Reference was made above to the complexation and hence polarization of the iodine by the thioethers thus facilitating the initial removal of H^- as HI from the cage (Scheme 3). Similar complex formation between iodine and ethers is also well documented.[12] In contrast, isocyanides RNC are known readily to react with halogens X_2 to form the corresponding *C*,*C*-dihaloimines RN=CX_2.[13] Indeed, it seems likely that the species $Bu^tN{=}CI_2$ may be involved in metal oxidation in the formation of **3**–**7** from **1** and **2**, and moreover could not abstract hydride from cage-boron vertices. These differences in behaviour towards iodine are the probable reason for the different reactivities and product types observed in the present systems.

In complexes **9**–**12** the iodine bridge between a boron atom in the metal-ligating CBBBB face of the CB_{10} fragment and the metal is as far as we are aware a structural feature not hitherto observed for a halogen ligand, though as mentioned above the existence of an intramolecular amino-bridge system has recently been established[6] in the anion [1,2-μ-$NHBu^t$-2,2,2-$(CO)_3$-*closo*-2,1-$MoCB_{10}H_{10}$]$^-$. In all the new compounds reported the metal has a filled 18-electron valence shell configuration though it is noteworthy that for **9**–**12** there are resonance forms depending on whether the donor bond is invoked between the iodine atom and the metal or the iodine atom and the cage-boron. Both formulations result in zwitterionic molecules with the latter arrangement corresponding to a uninegative cage system as in **13**–**16**. Derivatization of metallacarbaborane cage systems is a topic of current interest[2c] and the various complexes described here have potential as precursors to other species. Thus for species **8**–**16** the cyclic ether or sulfide groups should undergo ring opening reactions upon treatment with nucleophiles affording new cage substituted products.[3h]

Experimental

General

All reactions were carried out under an atmosphere of dry, oxygen-free nitrogen using standard Schlenk line techniques. Solvents were stored over and distilled from appropriate drying agents under nitrogen prior to use. Petroleum ether here refers to that fraction of boiling point 40–60 °C. Chromatography columns (typically *ca.* 15 cm in length and *ca.* 2 cm in diameter) were packed with silica gel (Acros, 60–200 mesh). NMR spectra were recorded at the following frequencies: ^{1}H 360.1, ^{13}C 90.6 and ^{11}B 115.5 MHz. Compounds **1**[3d] and **2**[3h] were prepared according to the literature.

Syntheses

Reactions of 1 and 2 with I_2 and $CNBu^t$. (i) A solution of **1** (0.52 g, 0.59 mmol) in CH_2Cl_2 (20 cm^3) was treated with $CNBu^t$ (0.27 cm^3, 2.39 mmol) followed by I_2 (0.15 g, 0.59 mmol), and the mixture was stirred for 12 h at ambient temperatures. The volatile components of the mixture were removed *in vacuo*, and the residue was redissolved in the minimum amount of CH_2Cl_2 (*ca.* 2 cm^3) and chromatographed. Elution with CH_2Cl_2–petroleum ether (2 : 1) gave a yellow fraction, which after removal of solvent *in vacuo* afforded yellow microcrystals of [2,2,2,2-$(CNBu^t)_4$-2-I-*closo*-2,1-$MoCB_{10}H_{11}$] **3** (0.38 g).

(ii) Similarly, the compound [2,2,2,2-$(CNBu^t)_4$-2-Br-*closo*-2,1-$MoCB_{10}H_{11}$] **4** (0.30 g) was obtained as yellow microcrystals from **1** and $CNBu^t$ as described for **3**, except that Br_2 (0.094 g, 0.59 mmol) was used instead of I_2.

(iii) Proceeding as in the synthesis of **3**, the reagents **1** with I_2 and $CNBu^t$ (0.13 cm^3, 1.15 mmol) gave yellow microcrystals of [2,2,2-$(CNBu^t)_3$-2-CO-2-I-*closo*-2,1-$MoCB_{10}H_{11}$] **5** (0.10 g).

(iv) Compound **2** (0.40 g, 0.41 mmol) was dissolved in CH_2Cl_2 (20 cm^3) and treated with $CNBu^t$ (0.19 cm^3, 1.68 mmol) and I_2 (0.11 g, 0.43 mmol) and the mixture stirred for 12 h. Solvent was removed *in vacuo* and the residue taken up in CH_2Cl_2 (*ca.* 1 cm^3) and applied to the top of a chromatography column. Elution with CH_2Cl_2–petroleum ether (1 : 1) gave a yellow fraction from which [2,2-$(CNBu^t)_2$-2,2-$(CO)_2$-2-I-*closo*-2,1-$WCB_{10}H_{11}$] **7** (0.048 g) was obtained as a yellow microcrystalline solid after removal of solvent *in vacuo*. Further elution with CH_2Cl_2–petroleum ether (2 : 1) then afforded a second yellow fraction which, after removal of solvent *in vacuo*, yielded yellow microcrystals of [2,2,2-$(CNBu^t)_3$-2-CO-2-I-*closo*-2,1-$WCB_{10}H_{11}$] **6** (0.096 g).

[$N(PPh_3)_2$][2,2,2-$(CO)_3$-2-I-7-{$O(CH_2)_4$}-*closo*-2,1-$MoCB_{10}H_{10}$]. Compound **1** (0.70 g, 0.80 mmol) was dissolved in THF (20 cm^3) and I_2 (0.20 g, 0.79 mmol) was added. After stirring for 12 h, solvent was removed *in vacuo*, and the residue dissolved in CH_2Cl_2 (*ca.* 2 cm^3) and chromatographed. Elution with

Table 3 Data for crystal structure analyses of compounds **3**·0.5CH_2Cl_2, **8**, **11a** and **14**·CH_2Cl_2[a]

	3·0.5CH_2Cl_2	**8**	**11a**	**14**·CH_2Cl_2
Chemical formula	$C_{21.5}H_{48}B_{10}ClIMoN_4$	$C_{44}H_{48}B_{10}IMoNO_4P_2$	$C_{10}H_{21}B_{10}IMoO_3S_3$	$C_{13}H_{27}B_{10}Cl_2IMoO_3S_4$
M	729.03	1047.71	616.39	761.43
Space group	$P2_1/c$	$P2_1/n$	$P2_1/n$	$P2_1/c$
a/Å	17.1449(14)	15.4517(14)	14.071(2)	8.8257(9)
b/Å	12.056(2)	10.669(2)	10.945(2)	10.6900(10)
c/Å	20.686(2)	29.866(3)	16.439(3)	30.297(4)
β/°	114.01(8)	97.233(14)	115.577(14)	95.612(10)
U/Å^3	3905.8(8)	4884.2(9)	2283.7(6)	2844.7(5)
μ(Mo-Kα)/cm^{-1}	12.12	10.07	22.10	20.45
T/K	173	293	293	173
Reflections measured	7092	6505	4150	5372
Independent reflections	6849	6286	3979	5021
R_{int}	0.0391	0.0673	0.0477	0.0345
$wR2$ (all data), $R1$[b]	0.0998, 0.0567	0.0997, 0.0499	0.0989, 0.0476	0.0980, 0.0526

[a] For all determinations, crystals were monoclinic with $Z = 4$. [b] $F_o > 4\sigma(F_o)$.

neat CH_2Cl_2 gave a red–brown eluate which, after evaporation of solvent *in vacuo*, afforded red–brown microcrystals of [N(PPh$_3$)$_2$][2,2,2-(CO)$_3$-2-I-7-{O(CH$_2$)$_4$}-*closo*-2,1-MoCB$_{10}$H$_{10}$] **8** (0.31 g).

Reactions of 1 with I_2 and sulfur donor ligands. (i) Compound **1** (0.30 g, 0.34 mmol) was dissolved in CH_2Cl_2 (20 cm^3). To this was added S(CH$_2$)$_4$ (0.030 cm^3, 0.34 mmol) followed by I_2 (0.088 g, 0.35 mmol), and the mixture was stirred at room temperature for 12 h. The more volatile components were removed *in vacuo*, and the residue redissolved in the minimum of CH_2Cl_2 (*ca.* 2 cm^3) and transferred to the top of a chromatography column. Elution first with CH_2Cl_2–petroleum ether (3 : 2) gave a purple fraction, from which was obtained a mixture of isomers of [2,2,2-(CO)$_3$-2,3-μ-I-*n*-{S(CH$_2$)$_4$}-*closo*-2,1-MoCB$_{10}$H$_9$] **9a** (n = 7) and **9b** (n = 11) (0.036 g total) as a purple microcrystalline solid following removal of solvent *in vacuo*. Further elution with CH_2Cl_2–petroleum ether (3 : 1) gave a brown fraction, from which the compound [2,2,2-(CO)$_3$-2-I-3,11-{S(CH$_2$)$_4$}$_2$-*closo*-2,1-MoCB$_{10}$H$_9$] **13** (0.048 g) was isolated as a tan powder after removal of solvent *in vacuo*.

(ii) Similarly, compound **1** with the reagents *cyclo*-1,4-S$_2$(CH$_2$)$_4$ (0.041 g, 0.34 mmol) and I_2 gave purple microcrystals of the mixture [2,2,2-(CO)$_3$-2,3-μ-I-*n*-{*cyclo*-1,4-S$_2$(CH$_2$)$_4$}-*closo*-2,1-MoCB$_{10}$H$_9$] **10a** (n = 7) and **10b** (n = 11) (0.040 g total), and dark red microcrystalline [2,2,2-(CO)$_3$-2-I-3,11-{*cyclo*-1,4-S$_2$(CH$_2$)$_4$}$_2$-*closo*-2,1-MoCB$_{10}$H$_9$] **14** (0.023 g).

(iii) By a similar method, purple microcrystalline [2,2,2-(CO)$_3$-2,3-μ-I-*n*-{*cyclo*-1,4,7-S$_3$(CH$_2$)$_6$}-*closo*-2,1-MoCB$_{10}$H$_9$] **11a** (n = 7) and **11b** (n = 11) (0.073 g total) and dark red microcrystalline [2,2,2-(CO)$_3$-2-I-3,11-{*cyclo*-1,4,7-S$_3$(CH$_2$)$_6$}$_2$-*closo*-2,1-MoCB$_{10}$H$_9$] **15** (0.065 g) were obtained by treatment of compound **1** with I_2 and *cyclo*-1,4,7-S$_3$(CH$_2$)$_6$ (0.061 g, 0.34 mmol).

(iv) Following a similar procedure to those by which compounds **9**–**11** and **13**–**15** were formed, compound **1** with I_2 and *cyclo*-1,4,7,10-S$_4$(CH$_2$)$_8$ (0.082 g, 0.34 mmol) gave only a single purple chromatographic fraction after chromatography, from which the mixture [2,2,2-(CO)$_3$-2,3-μ-I-*n*-{*cyclo*-1,4,7,10-S$_4$(CH$_2$)$_8$}-*closo*-2,1-MoCB$_{10}$H$_9$] **12a** (n = 7) and **12b** (n = 11) was obtained as a purple microcrystalline solid (0.11 g total).

[2,2,2-(CO)$_3$-2-I-3-{S(CH$_2$)$_4$}-11-{O(CH$_2$)$_4$}-*closo*-2,1-MoCB$_{10}$H$_9$]. To a solution of compound **8** (0.30 g, 0.29 mmol) in S(CH$_2$)$_4$ (20 cm^3) was added I_2 (0.073 g, 0.29 mmol) and the mixture was stirred for 12 h at ambient temperature. Solvent was removed *in vacuo*, the residue redissolved in the minimum of CH_2Cl_2 (*ca.* 2 cm^3) and this mixture chromatographed. An orange fraction was eluted with CH_2Cl_2–petroleum ether (2 : 1) from which [2,2,2-(CO)$_3$-2-I-3-{S(CH$_2$)$_4$}-11-{O(CH$_2$)$_4$}-*closo*-2,1-MoCB$_{10}$H$_9$] **16** (0.062 g) was obtained as a yellow–brown powder after removal of solvent *in vacuo*.

Crystallography

Experimental data for **3**, **8**, **11a** and **14** are given in Table 3; data for **15** are included in the ESI. Diffracted intensities were collected on an Enraf-Nonius CAD-4 diffractometer using graphite-monochromated Mo-Kα X-radiation. Final unit cell dimensions were determined from the setting angles of 25 accurately centered reflections. The data were corrected for Lorentz, polarization and X-ray absorption effects, the latter using a numerical method based on the measurements of crystal faces.

The structures were solved by direct methods and successive difference Fourier syntheses were used to locate all non-hydrogen atoms using SHELXTL version 5.03.[14] Refinements were made by full-matrix least squares on all F^2 data using SHELXL-97.[15] Anisotropic thermal parameters were included for all non-hydrogen atoms. For all structures, cage carbon atoms were assigned by comparison of the bond lengths to adjacent boron atoms in conjunction with the magnitudes of their isotropic thermal parameters. All hydrogen atoms were included in calculated positions and allowed to ride on their parent boron or carbon atoms with fixed isotropic thermal parameters [U_{iso}(H) = 1.2U_{iso}(parent) or U_{iso}(H) = 1.5U_{iso}(C) for methyl hydrogens].

The methyl groups on one of the CNBu^t ligands in **3** were disordered over two positions rotated approximately 45° from each other about the N(30)–C(31) bond axis. The occupancies of the major and minor components were restrained at 80 and 20%, respectively; the anisotropic thermal parameters of the analogous carbons in each set were assigned equivalent magnitudes.

Compound **3** co-crystallized with one half of a molecule of CH_2Cl_2 per asymmetric unit. One of the chlorine atoms was disordered over two sites and was refined with a fixed occupancy of 25% in each site. Compound **14** co-crystallized with one fully ordered dichloromethane molecule per formula unit which was refined without restraint. All calculations were carried out on Dell PC computers.

CCDC reference numbers (for **3**·0.5CH_2Cl_2, **8**, **11a** and **14**·CH_2Cl_2) 166146–166149.

See http://www.rsc.org/suppdata/dt/b1/b105158j/ for crystallographic data in CIF or other electronic format.

Acknowledgements

We thank the Robert A. Welch Foundation for support (Grant AA-1201).

References

1 D. E. Hyatt, J. L. Little, J. T. Moran, F. R. Scholer and L. J. Todd, *J. Am. Chem. Soc.*, 1967, **89**, 3342; W. H. Knoth, *J. Am. Chem. Soc.*, 1967, **89**, 3342; W. H. Knoth, *Inorg. Chem.*, 1967, **10**, 598; R. R. Rietz, D. F. Dustin and M. F. Hawthorne, *Inorg. Chem.*, 1974, **13**, 1580; C. G. Salentine and M. F. Hawthorne, *J. Am. Chem. Soc.*, 1975, **97**, 6382; W. E. Carroll, M. Green, F. G. A. Stone and A. J. Welch, *J. Chem. Soc., Dalton Trans.*, 1975, 2263.

2 (*a*) R. N. Grimes, in *Comprehensive Organometallic Chemistry*, ed. G. Wilkinson, E. W. Abel and F. G. A. Stone, Pergamon Press, Oxford, 1982, vol. 1, section 5.5; (*b*) R. N. Grimes, in *Comprehensive Organometallic Chemistry II*, ed. E. W. Abel, F. G. A. Stone and G. Wilkinson, Pergamon Press, Oxford, 1995, vol. 1 (ed. C. E. Housecroft), ch. 9; (*c*) R. N. Grimes, *Coord. Chem. Rev.*, 2000, **200–202**, 773.

3 (*a*) S. A. Batten, J. C. Jeffery, P. L. Jones, D. F. Mullica, M. D. Rudd, E. L. Sappenfield, F. G. A. Stone and A. Wolf, *Inorg. Chem.*, 1997, **36**, 2570; (*b*) I. Blandford, J. C. Jeffery, P. A. Jelliss and F. G. A. Stone, *Organometallics*, 1998, **17**, 1402; (*c*) J. C. Jeffery, P. A. Jelliss, L. H. Rees and F. G. A. Stone, *Organometallics*, 1998, **17**, 2258; (*d*) D. D. Ellis, A. Franken, P. A. Jelliss, F. G. A. Stone and P.-Y. Yu, *Organometallics*, 2000, **19**, 1993; (*e*) D. D. Ellis, A. Franken, P. A. Jelliss, J. A. Kautz, F. G. A. Stone and P.-Y. Yu, *J. Chem. Soc., Dalton Trans.*, 2000, 2509; (*f*) D. D. Ellis, A. Franken, T. D. McGrath and F. G. A. Stone, *J. Organomet. Chem.*, 2000, **614–615**, 208; (*g*) A. Franken, S. Du, P. A. Jelliss, J. A. Kautz and F. G. A. Stone, *Organometallics*, 2001, **20**, 1597; (*h*) S. Du, A. Franken, P. A. Jelliss, J. A. Kautz, F. G. A. Stone and P.-Y. Yu, *J. Chem. Soc., Dalton Trans.*, 2001, 1846.

4 D. D. Ellis, P. A. Jelliss and F. G. A. Stone, *Organometallics*, 1999, **18**, 4982; D. D. Ellis, P. A. Jelliss and F. G. A. Stone, *J. Chem. Soc., Dalton Trans.*, 2000, 2113; D. D. Ellis, J. C. Jeffery, P. A. Jelliss, J. A. Kautz and F. G. A. Stone, *Inorg. Chem.*, 2001, **40**, 2041.

5 (*a*) A. C. Filippou, W. Grünleitner and E. Herdtweck, *J. Organomet. Chem.*, 1989, **373**, 325; (*b*) A. G. Orpen, L. Brammer, F. H. Allen, O. Kennard, D. G. Watson and R. Taylor, *J. Chem. Soc., Dalton Trans.*, 1989, S1.

6 S. Du, T. D. McGrath, J. A. Kautz and F. G. A. Stone, *Inorg. Chem.*, 2001, **40**, in press.

7 W. R. Hertler, F. Klangberg and E. L. Mutterties, *Inorg. Chem.*, 1967, **6**, 1696; A. R. Siedle, D. McDowell and L. J. Todd, *Inorg. Chem.*, 1974, **13**, 2735.

8 J. Plesek, Z. Janousek and S. Hermanek, *Collect. Czech. Chem. Commun.*, 1978, **43**, 2862; W. Quintana and L. G. Sneddon, *Inorg. Chem.*, 1990, **29**, 3242.

9 M. F. Hawthorne, L. F. Warren, Jr., K. P. Callahan and N. F. Travers, *J. Am. Chem. Soc.*, 1971, **93**, 2407.

10 D. C. Young, D. V. Howe and M. F. Hawthorne, *J. Am. Chem. Soc.*, 1969, **91**, 859; H. C. Kang, S. S. Lee, C. B. Knobler and M. F. Hawthorne, *Inorg. Chem.*, 1991, **30**, 2024.

11 A. J. Blake, F. Cristiani, F. A. Devillanova, A. Garau, L. M. Gilby, R. O. Gould, F. Isaia, V. Lippolis, S. Parsons, C. Radek and M. Schröder, *J. Chem. Soc., Dalton Trans.*, 1997, 1337; A. J. Blake, F. A. Devillanova, A. Garau, L. M. Gilby, R. O. Gould, F. Isaia, V. Lippolis, S. Parsons, C. Radek and M. Schröder, *J. Chem. Soc., Dalton Trans.*, 1998, 2037, and references therein.

12 N. Baggett, in *Comprehensive Organic Chemistry*, ed. D. Barton and W. D. Ollis, Pergamon Press, Oxford, 1979, vol. 1 (ed. J. F. Stoddart), ch. 4.3; A. N. Haines, in *Comprehensive Organic Chemistry*, ed. D. Barton and W. D. Ollis, Pergamon Press, Oxford, 1979, vol. 1 (ed. J. F. Stoddart), ch. 4.4.

13 G. Tennant, in *Comprehensive Organic Chemistry*, ed. D. Barton and W. D. Ollis, Pergamon Press, Oxford, 1979, vol. 2 (ed. I. O. Sutherland), ch. 8.

14 SHELXTL version 5.03, Bruker AXS, Madison, WI, 1995.

15 G. M. Sheldrick, University of Göttingen, Germany, 1997.